Morpho-molecular Characterization of the Litostomatean Predatory Ciliate Phialina pupula (Müller, 1773) Foissner

Article *in* Acta Protozoologica · July 2019

DOI: 10.4467/16890027AP.19.004.10835

CITATIONS
6

READS
783

3 authors:

Ľubomír Rajter
University of Duisburg-Essen
36 PUBLICATIONS **206** CITATIONS
SEE PROFILE

William A Bourland
Charles University in Prague
146 PUBLICATIONS **1,809** CITATIONS
SEE PROFILE

Peter Vďačný
Comenius University Bratislava
215 PUBLICATIONS **1,943** CITATIONS
SEE PROFILE

DOI: 10.4467/16890027AP.19.004.10835

Morpho-molecular Characterization of the Litostomatean Predatory Ciliate *Phialina pupula* (Müller, 1773) Foissner, 1983 (Haptoria, Lacrymariidae)

Ľubomír RAJTER[1], William BOURLAND[2], Peter VĎAČNÝ[1]

[1]Comenius University in Bratislava, Department of Zoology, Bratislava, Slovak Republic; [2]Boise State University, Department of Biological Sciences, Boise, Idaho, U.S.A.

Address for correspondence: Peter Vďačný, Department of Zoology, Faculty of Natural Sciences, Comenius University in Bratislava, Ilkovičova 6, 842 15 Bratislava, Slovak Republic; E-mail: peter.vdacny@uniba.sk

Figures: 6
Tables: 1
Supplementary Tables: 3

Abstract. The morphology and phylogenetic position of a haptorian ciliate, *Phialina pupula* (Müller, 1773) Foissner, 1983, isolated from microaerobic sandy sediments of the floodplain area of the Boise River, Idaho, U.S.A., were studied using live observation, protargol impregnation, scanning electron microscopy, and the 18S rRNA gene as well as the ITS region. The Boise population of *P. pupula* is characterized by a size of about 60–130 × 20–50 µm, an elliptical macronucleus with a single micronucleus, highly refractive dumbbell-shaped inclusions scattered throughout the cytoplasm and concentrated in the anterior body half, a single subterminal/terminal contractile vacuole, about 10 µm long rod-shaped extrusomes, and an average of 15 ciliary rows. In phylogenetic analyses, the newly obtained sequences from *P. pupula* and *Lacrymaria olor* clustered within the family Lacrymariidae with full to moderate statistical support. Neither the genus *Phialina* nor the genus *Lacrymaria* was depicted monophyletic both in the single gene and multigene phylogenetic inferences. Specifically, the genus

DOI: 10.4467/16890027AP.19.004.10835

Phialina was shown as a paraphyletic assemblage containing members of the polyphyletic genus *Lacrymaria*. This indicates that the phialinid bauplan, i.e., an anterior body end differentiated into a head-like structure directly attached to the trunk, might represent the ground pattern in the family Lacrymariidae. On the other hand, the long highly contractile neck carrying the head-like structure probably evolved later and convergently in multiple *Lacrymaria* species from *Phialina*-like ancestors.

Keywords: 18S rRNA gene; Boise; Floodplain sand; ITS region; Lacrymariidae; Phylogeny

INTRODUCTION

Phialina pupala (Müller, 1773) Foissner, 1983 represents a free-living, predatory ciliate belonging to the subclass Haptoria Corliss, 1974 of the highly diverse class Litostomatea Small and Lynn, 1981. Müller (1773) described this species for the first time as a cone-shaped microorganism with an apical head-like structure. Later on, Bory de Saint-Vincent (1824) classified all ciliates with an apical head into the genera *Phialina* Bory de Saint-Vincent, 1824 and *Lacrymaria* Bory de Saint-Vincent, 1824. He distinguished the two genera by the localization of the cell mouth: *Phialina* has a lateral while *Lacrymaria* possesses a terminal cytostome. These generic characters were, however, revealed to be problematic and consequently most species were assigned to *Lacrymaria* (Ehrenberg 1838, Dujardin 1841, Claparède and Lachmann 1859, Fromentel 1874, Bütschli 1887–89, Penard 1922). Kahl (1930) noticed that all species with an apical head have only a terminal cell mouth. This showed the main diagnostic feature of the genus *Phialina* to be incorrect. Therefore, Kahl (1930) abandoned the genus name *Phialina* and used only the generic name *Lacrymaria*. In spite of this, *Phialina* was resurrected and both genera were redefined as follows (Foissner 1983, Foissner *et al.* 1995): (i) *Lacrymaria* is highly contractile and has a conspicuously long, highly extensible, swan-like neck (Fig. 1A) while (ii) *Phialina* is less contractile and does not have a distinct extensible neck but, instead, the head is attached directly to the trunk (Fig. 1B). With the aid of silver staining methods, two further lacrymariid genera were established (Foissner 1988, Foissner *et al.* 1999): *Phialinides* Foissner, 1988 with a monokinetidal circle (paratene) between the head and the trunk (Fig. 1C) and *Pelagolacrymaria* Foissner *et al.*, 1999 in which this circle (paratene) is composed of dikinetids. The application of sophisticated staining methods thus leads not only to a more accurate characterization of new lacrymariid species (Berger *et al*. 1984;

DOI: 10.4467/16890027AP.19.004.10835

Foissner 1984, 1988, 2016; Foissner *et al.* 2002; Wang *et al*. 2019) and comprehensive re-descriptions of several insufficiently known species (Foissner 1983, Foissner *et al*. 2002, Foissner and Wenzel 2004, Wang *et al*. 2019), but also to discovery of new genera (Foissner 1988, Foissner *et al.* 1999).

According to molecular data, *Phialina* and *Lacrymaria* form a monophyletic group, the family Lacrymariidae Fromentel, 1876, but the phylogenetic position of the family within the class Litostomatea remains unresolved (Gao *et al*. 2008, Vďačný *et al*. 2011, Zhang *et al*. 2012, Kwon *et al*. 2014, Vďačný and Rataj 2017, Wu *et al*. 2017, Huang *et al*. 2018, Wang *et al*. 2019). Neither the genus *Phialina* nor the genus *Lacrymaria* is monophyletic and their species are intermingled in single gene and also in multigene phylogenies (Wu *et al*. 2017, Huang *et al*. 2018, Wang *et al*. 2019). This fact indicates that a new taxonomic concept is needed to reconcile the conflicts between morphologic and molecular classifications.

Although notable progress has been achieved in the morphological and molecular research on the family Lacrymariidae in the past 35 years, there are still many "old" species that need to be investigated using modern alpha-taxonomic methods. Moreover, the molecular sampling of lacrymariids is also limited and sequences from more taxa and genes are needed to reconstruct the evolutionary history of this peculiar group of predatory ciliates more robustly. Therefore, we provide in this study a comprehensive morphological re-description of an insufficiently known species, *P. pupula*, and multigene phylogenetic analyses of the family Lacrymariidae.

MATERIAL AND METHODS

Sampling, morphologic methods and terminology

Populations of *P. pupula* and *Lacrymaria olor* (Müller, 1786) Bory de Saint-Vincent, 1824 were collected in Boise, Idaho, northwestern U.S.A. (Supplementary Table S1). The former species was isolated from sand percolates of the floodplain area of the Boise River near the Glenwood Bridge (43°39'47.57" N, 116°16'56.99" W). The latter species was gathered from sediments of a pond in the Julia Davis Park (43°36'23.84" N, 116°11'46.24" W). Both species were isolated directly from the environmental samples after transportation to the laboratory at Boise State University.

Living specimens were studied using a Zeiss Axioskop 2 Plus microscope at 100–1000× magnification. Protargol impregnation was carried following the Wilbert's method (Ji and Wang 2018). Specimens for scanning electron microscopy (SEM) were prepared according to Foissner (2014).

DOI: 10.4467/16890027AP.19.004.10835

Briefly, ciliates were fixed with 1:1 solution of 2.5% glutaraldehyde and 2% osmium tetroxide, dehydrated in ethanol (50, 70, 90 and three changes of 100%), dried in a critical point dryer (EMS 850, Electron Microscopy Sciences, Hatfield, PA, USA), sputtered with gold in an Agar sputter coater (Electron Microscopy Sciences, Hatfield, PA, USA), and examined at 15 kV in a Hitachi S-3400N scanning electron microscope (Hitachi High-Technologies Corporation, Tokyo, Japan). Living specimens were measured from images captured with a Flex Digital camera (Diagnostic Instruments, Sterling Heights, MI) using the calibrated software ImageJ (Schneider *et al.* 2012). Protargol-impregnated cells were measured directly under the optical microscope using an ocular micrometer. Illustrations of live specimens and impregnated cells were based on microphotographs. Unfortunately, the quality of *L. olor* preparations was insufficient for a thorough morphologic description. Therefore, we morphologically characterize only *P. pupula* in detail here but provide sequence data for both species.

General terminology follows Lynn (2008) and specific terminology is according to Foissner and Xu (2007) as well as Vďačný and Foissner (2012).

Molecular methods

After identification, several specimens from both species were picked, washed and transferred into the cell lysis buffer. The DNEasy Blood & Tissue Kit (Qiagen, Hildesheim, Germany) was used to extract the genomic DNA. Amplification of the 18S rRNA gene followed Vďačný *et al*. (2011) while that of the ITS1-5.8S-ITS2 region was according to Vďačný *et al*. (2012). PCR products were enzymatically purified and ligated into a plasmid with the pGEM®-T and pGEM®-T Easy Vector Systems (Promega, Madison, Wisconsin, USA). After a 12-hour incubation of the ligation mixture at 4 °C, recombinant plasmids were introduced into the competent *Escherichia coli* cells (strain JM109). The efficiency of transformation was checked by the blue-white selection method. Molecularly cloned recombinant plasmids were again subjected to PCR but using the M13F and M13R primers under the same conditions as described in Vďačný *et al*. (2011). The resulting PCR products were enzymatically purified and then sequenced on an ABI 3730 automatic sequencer (Macrogen Inc., Amsterdam, The Netherlands) using the M13F and M13R primers.

Sequences and phylogenetic analyses

The obtained sequence fragments were checked, trimmed and assembled into contigs using BioEdit

DOI: 10.4467/16890027AP.19.004.10835

ver. 7.2.5 (Hall 1999). All 18S rRNA gene and ITS1-5.8S-ITS2 region sequences were deposited in the GenBank database. Their length, GC content and GenBank accession numbers are provided in Supplementary Table S1. Multi-sequence alignments were constructed using the MAFFT algorithm and were masked with the cutoff value of 0.93 (Supplementary Table S2) on the Guidance2 server (http://guidance.tau.ac.il/ver2/) (Sela *et al.* 2015).

Maximum likelihood and Bayesian inference were used to analyze ten alignments, as specified in Supplementary Table S2. The best evolutionary substitution models under the Akaike information criterion were selected using jModelTest ver. 0.1.1 (Guindon and Gascuel 2003, Posada 2008). Parameters of the best fitting substitution models for both Bayesian and maximum likelihood analyses were summarized in Supplementary Table S2. Maximum likelihood analyses were conducted with PhyML ver. 3.0 on the South of France bioinformatics platform (http://www.atgc-montpellier.fr/phyml/) (Guindon *et al*. 2010) using the SPR tree-rearrangement and one thousand non-parametric bootstrap replicates. Following Hillis and Bull (1993), bootstrap values <70% were considered as low, 70–94% as moderate, and ≥95% as high. Bayesian inference was performed with MrBayes ver. 3.2.6 (Ronquist *et al*. 2012) on the CIPRES Portal ver. 3.1 (http://www.phylo.org), using four independent chains, five million generations and a sampling frequency of one thousand. The burn-in fraction was specified as 25% of the first sampled trees. Posterior probabilities <0.94 were consider as low while ≥95 as high (Alfaro *et al*. 2003). Bayesian and maximum likelihood trees were visualized in FigTree ver. 1.2.3 (Rambaut 2009).

RESULTS

Phialina pupula (Müller, 1773) Foissner, 1983

Zoobank registration number: urn:lsid:zoobank.org:pub:BFF7D5C4-A4F7-42F9-9FCC-DBE7814F0000.

Improved diagnosis (based on Boise population): In vivo size about 60–130 × 20–50 µm. Body shape highly variable depending on state of contraction, ranging from clavate in extended condition through fusiform, obpyriform, elliptical to almost globular in semi-contracted and contracted state. Macronucleus elliptical with a single micronucleus. Highly refractive dumbbell-shaped inclusions scattered throughout cytoplasm and usually concentrated in anterior body part. Contractile vacuole subterminal in extended condition, terminal in contracted state. Extrusomes about 10 µm long, rod-

DOI: 10.4467/16890027AP.19.004.10835

shaped, attached to oral bulge and forming bundles in cytoplasm. On average 15 ciliary rows, each row anteriorly differentiated into a dorsal brush composed of one to four dikinetids.

Type locality: Müller (1773) did not specify the type locality. He mentioned only that he found the species in water and ice from dunghills during November and December.

Type material and voucher slides: No type material is available from Müller's (1773) specimens. Three voucher slides containing protargol-impregnated specimens from the Boise population have been deposited at Department of Zoology, Comenius University in Bratislava.

Material studied: Specimens from lower microaerobic layers of the interstitial sandy sediments from the floodplain area of the Boise River near the Glenwood Bridge, Boise, Idaho, U.S.A.

Etymology: Not given in the original description. The feminine Latin noun *pupula* is a diminutive form of *pupa* (doll, puppet or pupa of an insect), obviously referring to the doll- or pupa-like body shape of the ciliate. The name is treated as a noun in the nominative singular standing in apposition to the generic name [Art. 11.9.1.2 of the International Commission on Zoological Nomenclature (1999)].

Description of Boise population: Size in vivo 60–130 × 20–50 μm, usually about 85 × 30 μm, as calculated from some in vivo measurements and morphometric data adding 15% preparation shrinkage; length:width ratio on average 2.2:1 in vivo and 2.9:1 (n = 32) in protargol preparations (Table 1). Body shape highly variable depending on state of contraction, ranging from clavate in extended condition through fusiform, obpyriform, elliptical to almost globular in semi-contracted and contracted state. Head barrel-shaped, about 8.5 × 6.0 μm in size after protargol impregnation, distinct from trunk but without neck-like region, sometimes retracted into trunk creating an impression of shoulders. Posterior body end tapered and tail-like in extended condition, narrowly to broadly rounded in semi-contracted and contracted state (Figs 2A, E, F, 3A, C, E, F, H–M). Contraction occurs slowly.

Nuclear apparatus located in or slightly posterior to mid-body, usually slightly lateral of cell center. Macronucleus elliptical, on average 15 × 10 μm (n = 32) in size after protargol impregnation. Micronucleus adjacent to macronucleus, usually attached to anterior pole of macronucleus, elliptical and about 2 μm long in vivo (Table 1; Figs 2A, 3A, D, E, F). Contractile vacuole subterminal in extended specimens while terminal in semi-contracted and contracted cells, excretory pore(s) not recognizable in vivo or after protargol impregnation (Figs 2A, F, 3A, F). Only one type of extrusomes, rod-shaped, about 10 × 0.5 μm in size in vivo, attached to oral bulge and in bundles scattered throughout cytoplasm, impregnate well with the protargol method used (Figs 2A, C, 3C, F, G). Cortex very flexible, distinctly furrowed by ciliary rows, sometimes dotted by tips of cortical granules in SEM

DOI: 10.4467/16890027AP.19.004.10835

(Fig. 4A–C). Cortical granules colorless, broadly elliptical to elliptical and about 0.8 × 0.4 μm in size in vivo, oriented perpendicularly to cell surface, rather irregularly and narrowly spaced forming seven or eight rows between adjacent ciliary rows, impregnate deeply with the protargol method used often making observations of the ciliary pattern difficult (Figs 2D, 3A, F). Cytoplasm colorless, packed with few to many lipid droplets, some extrusome bundles, and many highly refractive inclusions. Individual inclusions dumbbell-shaped, about 2 μm long and usually numerous in anterior body half, rendering the cell dark in appearance at low magnifications (Figs 2A, B, 3A–C, E–M). Swims fast along helical trajectory by rotation about main body axis.

Somatic cilia about 8 μm long in vivo, arranged in an average of 15 rows, each row composed of about 22 monokinetids with some dikinetids (dividing basal bodies) irregularly interspersed. Somatic kineties ordinarily spaced, extend meridionally to slightly helically depending on state of contraction (Table 1; Figs 2A, 4A, C). Dorsal brush at anterior end of all somatic kineties, very inconspicuous not only in vivo but also in protargol preparations and in SEM because composed of only two to five dikinetids (SEM measurements): first brush dikinetid bears a short, 1.5–2.0 μm-long, rod-like cilium followed by an ordinary cilium about 6.5 μm long; second dikinetid associated with a minute, 0.3 μm-long, stump-like cilium followed by an ordinary cilium; all following brush dikinetids with anterior basal body unciliated and posterior basal body bearing an ordinary cilium (Table 1; Figs 2E, 4A, B).

Oral apparatus occupies apical end of head. Oral bulge contains tip of extrusomes, posteriorly delimited by circumoral kinety as usual in congeners. Circumoral kinety and its structure very difficult to recognize in protargol preparations, very likely composed of dikinetids. Head kineties helical and narrowly spaced, extend between circumoral kinety and dorsal brush, composed of densely arranged monokinetids bearing about 10 μm long cilia in vivo and almost completely covering head in SEM (Figs 2A, E, 3A, 4A).

Phylogenetic analyses

In total, ten alignments containing 18S rRNA gene sequences, ITS region sequences and their concatenations, were analyzed using Bayesian inference and maximum likelihood (Supplementary Table S2). Six alignments contained representatives of all main litostomatean lineages and members of the class Armophorea served to root the trees. The remaining four alignments included only sequences from representatives of the family Lacrymariidae. To test the robustness of results, each unmasked alignment has its counterpart masked with a cutoff value of 0.93. All analyses resulted in similar

DOI: 10.4467/16890027AP.19.004.10835

topologies with respect to statistically supported nodes. Therefore, we present here only trees inferred from the unmasked concatenated 18S rRNA gene-ITS region dataset containing 80 litostomatean taxa (Fig. 5) and from the masked 18S rRNA gene alignment containing 22 lacrymariid taxa (Fig. 6).

The class Litostomatea was recognized as a monophyletic group with full statistical support. The order Helicoprorodontida and the family Chaeneidae were placed as deep-branching lineages but the statistical support for their positions was weak in the maximum likelihood analyses, very likely because of long branch attraction. Relationships among the remaining litostomateans were poorly resolved although the main lineages were usually strongly statistically supported. Rhynchostomatians formed a fully statistically supported cluster both in the Bayesian and the maximum likelihood tree. Haptorians with one- or two-rowed dorsal brush and meridionally extending somatic kineties (Pleurostomatida, Homalozoonidae, and Haptorida) were clustered together in the Bayesian inference tree with high statistical support but this group was not corroborated in the maximum likelihood analyses. The order Spathidiida was depicted as paraphyletic, containing endocommensals from the subclass Trichostomatia, and this whole assemblage received full statistical support in the Bayesian tree but very low statistical support in the maximum likelihood tree. The family Lacrymariidae was fully to moderately statistically supported and was placed in a polytomy of the subclass Haptoria (Fig. 5).

Evolutionary relationships among members of the family Lacrymariidae were investigated in detail on the basis of the 18S rRNA gene (Fig. 6). Neither the genus *Phialina* nor the genus *Lacrymaria* were monophyletic. The genus *Phialina* was depicted as paraphyletic containing the polyphyletic genus *Lacrymaria*. The newly obtained *P. pupula* sequences formed a fully supported clade that was placed at the very base of the Lacrymariidae. Two variably supported *Phialina* clusters were further recognized: (i) the *P. caudata* + *P. clampi* + *Phialina* sp. MF474346 group and (ii) the *P. salinarum* + *P. vertens* + *Phialina* sp. FJ870088 and FJ876972 group. The latter group was depicted as sister to the *L. marina* + *L. maurea* + *L. olor* + Lacrymariidae sp. assemblage. Only *Lacrymaria* sp. 1 did not cluster with congeners, causing the polyphyly of the genus *Lacrymaria* (Fig. 6). However, *Lacrymaria* sp. 1 clusters with the other *Lacrymaria* species when more molecular characters are included (e.g. Huang *et al.* 2018).

DISCUSSION

Comparison of *Phialina pupula* populations

DOI: 10.4467/16890027AP.19.004.10835

Müller (1773) described *P. pupula* very briefly and without illustration under the name *Enchelis pupula*. Later, Müller (1786) provided a description with figures that, however, did not enable unambiguous identification of the species. Multiple descriptions of populations identified as *P. pupula* occur sporadically in the literature, for instance, in Kahl (1930), Gajewskaja (1933), Dragesco (1960), Vuxanovici (1963) as well as in Song and Wilbert (1989). All basically match in the body shape, the nuclear and contractile vacuole apparatus as well as in the extrusome pattern. However, most authors very likely depicted only semi-contracted, mostly elliptical specimens with a rounded posterior body end. The single exception is the study of Vuxanovici (1963) who described and illustrated almost the whole range of shape variability, including obconical, obpyriform, elliptical and even sigmoidal cells.

Kahl (1930) described very peculiar dumbbell-shaped inclusions scattered throughout the cytoplasm and especially concentrated in the anterior body half of *P. pupula*. Gajewskaja (1933) illustrated these remarkable inclusions in her specimens and we also observed them in the Boise exemplars. However, they were not present in every cell, which possibly explains why these dumbbell-shaped inclusions were not mentioned by Vuxanovici (1963).

Some *P. pupula* populations differ in two taxonomically important features, the body size and the number of the ciliary rows, indicating that they might be not conspecific. Specifically, Kahl's (1930) specimens were 120–180 µm long, Dragesco's (1960) individuals were 160 µm long, Gajewskaja's (1933) as well as Song and Wilbert's (1989) exemplars were only 60–90 µm long, and Vuxanovici (1963) did not mention the length at all. By contrast, Boise specimens were within the range provided by Kahl (1930) and Gajewskaja (1933) as well as Song and Wilbert (1989), i.e., they measured 60–130 × 20–50 µm, usually about 85 × 30 µm. Nevertheless, we cannot exclude that *P. pupula* is highly variable in body size, possibly reflecting contractility and nutritional factors. Indeed, the body length in phialinids usually spans a comparatively wide range (e.g., Foissner 1983, Foissner *et al*. 2002, Wang *et al*. 2019). *Phialina pupula* populations also differ conspicuously in the number of ciliary rows. There are about eight rows on one side according to Kahl (1930) and ten rows on one side according to Gajewskaja (1933) but 30 rows in total according Dragesco (1960) and 43–52 rows in total according to Song and Wilbert (1989). Boise specimens display about eight ciliary rows on one side, matching Kahl's (1930) and Gajewskaja's (1933) observations quite well.

To summarize, the Boise population might be conspecific with *P. pupula* sensu Kahl (1930), Gajewskaja (1933) and Vuxanovici (1963). However, *P. pupula* sensu Dragesco (1960) and Song and Wilbert (1989) very likely represent a different species due to the markedly higher number of ciliary

DOI: 10.4467/16890027AP.19.004.10835

rows.

Comparison of *Phialina pupula* with similar species

Phialina pupula can be easily distinguished from all congeners by having highly refractive dumbbell-shaped inclusions scattered throughout the cytoplasm and usually concentrated in the anterior body half (Kahl 1930, Gajewskaja 1933, present study). Interestingly, Kahl (1930) observed dark granules also in *P. coronata* (Claparède and Lachmann, 1859) Foissner, 1987 but, as he explicitly mentioned, they were never dumbbell-shaped. Moreover, *P. coronata* occurs in salt water in contrast to the freshwater *P. pupula* (Kahl 1930, Foissner *et al.* 1995).

There are three freshwater species, viz., *P. vermicularis* (Müller, 1786) Bory de Saint-Vincent, 1824, *P. vertens* (Stokes, 1885) Foissner and Adam, 1979 and *Lacrymaria phialina* Švec, 1897, which resemble *P. pupula* in body shape, characteristics of the nuclear and contractile vacuole apparatus, and the extrusome pattern. *Phialina vermicularis*, as redescribed by Foissner (1983), also differs from *P. pupula* in body length (40–60 µm vs. 60–180 µm) and the shape of the cortical granules (conspicuous and rod-shaped vs. inconspicuous and broadly elliptical to elliptical). *Phialina vertens*, as redescribed by Foissner (1983), is distinguished from *P. pupula* by the contractile vacuole surrounded by slightly yellowish granules. And, finally, *L. phialina*, as re-described by Penard (1922), has almost twice the number of ciliary rows as *P. pupula* (about 30 vs. 15).

Molecular and morphological evolution of the family Lacrymariidae

According to multiple phylogenetic analyses, the family Lacrymariidae represents a monophyletic and distinct lineage within the subclass Haptoria (e.g., Gao *et al*. 2008, Vďačný *et al*. 2011, Zhang *et al*. 2012, Kwon *et al*. 2014, Wu *et al*. 2017, Huang *et al*. 2018, Wang *et al*. 2019), which is also in accordance with the present results (Figs 5, 6). In the pioneer studies, the genera *Phialina* and *Lacrymaria* were each depicted as being monophyletic (Zhang *et al*. 2012, Kwon *et al*. 2014). However, with an increasing sequence pool, both genera have become non-monophyletic (Wu *et al*. 2017, Huang *et al*. 2018, Wang *et al*. 2019, present study). Although the generic home of most lacrymariid taxa is questionable and unstable (e.g., Penard 1922, Kahl 1930, Foissner 1983, Dragesco and Dragesco-Kernéis 1986, Foissner *et al.* 1995, Jankowski 2007), *Phialina* appears to be a paraphyletic stem genus while *Lacrymaria* seems to be polyphyletic both in the single gene and multigene phylogenetic analyses (Figs 5, 6). Therefore, we suppose that the phialinid bauplan, i.e., the anterior body end differentiated

DOI: 10.4467/16890027AP.19.004.10835

into a head-like structure directly attached to the trunk (i.e. without an intervening neck-like region), might represent the ground pattern in the family Lacrymariidae. On the other hand, the long highly contractile neck carrying the head-like structure probably evolved later and convergently in multiple *Lacrymaria* species from *Phialina*-like ancestors.

The phylogenetic home of the family Lacrymariidae within the subclass Haptoria is still uncertain (for details, see Vďačný and Rataj 2017). However, the peculiar brush structure of the family Lacrymariidae, i.e., the posterior basal body of brush dikinetids associated with an ordinary cilium (Fig. 4A, B), indicates a close relationship with the family Chaeneidae Kwon *et al.*, 2014. There are also further morphological features (e.g., body contractility, head-like anterior body end, and separation of the dorsal brush from the anterior body end by files of somatic monokinetids) corroborating the sister-group relationship of the families Lacrymariidae and Chaeneidae (Kwon *et al.* 2014, Vďačný and Rataj 2017). Whether these features are synapomorphies, plesiomorphies or homoplasies, needs to be tested by further molecular markers.

Acknowledgements. This work was supported by the Slovak Research and Development Agency under the contract No. APVV-15-0147 and by the Grant Agency of the Ministry of Education, Science, Research and Sport of the Slovak Republic and Slovak Academy of Sciences under the Grant VEGA 1/0041/17.

REFERENCES

Alfaro M. E., Zoller S., Lutzoni F. (2003) Bayes or bootstrap? A simulation study comparing the performance of Bayesian Markov Chain Monte Carlo sampling and bootstrapping in assessing phylogenetic confidence. *Mol. Biol. Evol.* **20:** 255–266

Berger H., Foissner W., Adam H. (1984) Taxonomie, Biometrie und Morphogenese einiger terricoler Ciliaten (Protozoa: Ciliophora). *Zool. Jb. Syst.* **111:** 339–367

Bory de Saint-Vincent J. B. (1824) Encyclopédie méthodique. Histoire Naturelle des zoophytes, ou animaux rayonnés, fainsant suite a l'histoire naturelle des vers de bruguière. Tome second. Aggase, Paris

Bütschli O. (1887–1889) Erster Band Protozoa. III Abteilung: Infusoria und System der Radiolaria. In: Klassen und Ordnungen des Thier-Reichs, Vol. I., (Ed. H. G. Bronn). C. F. Winter'sche

DOI: 10.4467/16890027AP.19.004.10835

Verlagshandlung, Leipzig, Heidelberg, 1098–2035

Claparède É., Lachmann J. (1859) Études sur les infusoires et les rhizopodes. *Mém. Inst. Natn. Génev.* **6** (year 1858): 261–482

Corliss J. O. (1974) The changing world of ciliate systematics: historical analysis of past efforts and a newly proposed phylogenetic scheme of classification for the protistan phylum Ciliophora. *Syst. Zool.* **23:** 91–138

Dragesco J. (1960) Ciliés mésopsammiques littoraux. Systématique, morphologie, écologie. *Trav. Stn. Biol. Roscoff (N. S.)* **12:** 1–356

Dragesco J., Dragesco-Kernéis A. (1986) Ciliés libres de l'Afrique intertropicale. Introduction à la connaissance et à l'étude des ciliés. *Faune tropicale* **26:** 1–559

Dujardin F. (1841) Histoire naturelle des zoophytes. Infusoires. Libraire Encyclopédique de Roret, Paris

Ehrenberg C. G. (1838) Die Infusionsthierchen als vollkommene Organismen. Ein Blick in das tiefere organische Leben der Natur. Verlag von Leopold Voss, Leipzig

Foissner W. (1983) Taxonomische Studien über die Ciliaten des Großglocknergebietes (Hohe Tauern, Österreich) I. Familien Holophryidae, Prorodontidae, Plagiocampidae, Colepidae, Enchelyidae und Lacrymariidae nov. fam. *Ann. Nat. Hist. Mus. Wien Ser. B Bot. Zool.* **84:** 49–85

Foissner W. (1984) Infraciliatur, Silberliniensystem und Biometrie einiger neuer und wenig bekannter terrestrischer, limnischer und mariner Ciliaten (Protozoa: Ciliophora) aus den Klassen Kinetofragminophora, Colpodea und Polyhymenophora. *Stapfia* **12:** 1–165

Foissner W. (1987) Miscellanea Nomenclatorica Ciliatea (Protozoa: Ciliophora). *Arch. Protistenkd.* **133:** 219–235

Foissner W. (1988) Gemeinsame Arten in der terricolen Ciliatenfauna (Protozoa: Ciliophora) von Australien und Afrika. *Stapfia, Linz,* **17:** 85–133

Foissner W. (2014) An update of 'basic light and scanning electron microscopic methods for taxonomic studies of ciliated protozoa'. *Int. J. Syst. Evol. Microbiol.* **64:** 271–292

Foissner W. (2016) Protists as bioindicators in activated sludge: Identification, ecology and future needs. *Eur. J. Protistol.* **55:** 75–94

Foissner W., Adam H. (1979) Die Bedeutung der stagnierenden Kleingewässer im alpinen Ökosystem. *Jb. Univ. Salzburg* **1977–1979:** 147–158

Foissner W, Wenzel F. (2004) Life and legacy of an outstanding ciliate taxonomist, Alfred Kahl (1877–1946), including a facsimile of his forgotten monograph from 1943. *Acta Protozool.* (Suppl.) **43:** 3–

DOI: 10.4467/16890027AP.19.004.10835

69

Foissner W., Xu K. (2007) Monograph of the Spathidiida (Ciliophora, Haptoria). Vol. I: Protospathidiidae, Arcuospathidiidae, Apertospathulidae. Springer-Verlag, Dordrecht

Foissner W., Berger H., Blatterer H., Kohmann F. (1995) Taxonomische und ökologische Revision der Ciliaten des Saprobiensystems – Band IV: Gymnostomatea, *Loxodes*, Suctoria. Informationsberichte des Bayerischen Landesamtes für Wasserwirtschaft, Deggendorf

Foissner W., Berger H., Schaumburg J. (1999) Identification and ecology of limnetic plankton ciliates. Informationsberichte des Bayerischen Landesamtes für Wasserwirtschaft, Deggendorf

Foissner W., Agatha S., Berger H. (2002) Soil ciliates (Protozoa, Ciliophora) from Namibia (southwest Africa) with emphasis on two contrasting environments, the Etosha region and the Namib Desert. Denisia **5:** 1–1459

Fromentel E. de (1874–1876) Études sur les microzoaires ou infusoires proprement dits comprenant de nouvelles recherches sur leur organisation, leur classification et la description des espèces nouvelles ou peu connus. G. Masson, Paris

Gajewskaja N. (1933) Zur Oekologie, Morphologie und Systematik der Infusorien des Baikalsees. *Zoologica, Stuttg.* **32:** 1–298

Gao S., Song W., Ma H., Clamp J. C., Yi Z., Al-Rasheid K. A. S., Chen Z., Lin X. (2008) Phylogeny of six genera of the subclass Haptoria (Ciliophora, Litostomatea) inferred from sequences of the gene coding for small subunit ribosomal RNA. *J. Eukaryot. Microbiol.* **55:** 562–566

Guindon S., Gascuel O. (2003) A simple, fast, and accurate algorithm to estimate large phylogenies by maximum likelihood. *Syst. Biol.* **52:** 696–704

Guindon S., Dufayard J. F., Lefort V., Anisimova M., Hordijk W., Gascuel O. (2010) New algorithms and methods to estimate maximum-likelihood phylogenies: assessing the performance of PhyML 3.0. *Syst. Biol.* **59:** 307–321

Hall T. A. (1999) BioEdit: a user-friendly biological sequence alignment editor and analysis program for Windows 95/98/NT. *Nucleic Acids Symp. Ser.* **41:** 95–98

Hillis D. M., Bull J. J. (1993) An empirical test of bootstrapping as a method for assessing confidence in phylogenetic analysis. *Syst. Biol.* **42:** 182–192

Huang J. B., Zhang T., Zhang Q., Li Y., Warren A., Pan H., Yan Y. (2018) Further insights into the highly derived haptorids (Ciliophora, Litostomatea): phylogeny based on multigene data. *Zool. Scr.* **47:** 231–242

DOI: 10.4467/16890027AP.19.004.10835

International Commission on Zoological Nomenclature [ICZN] (1999) International Code of Zoological Nomenclature. 4th ed. Tipografia La Garangola, Padova

Jankowski A. W. (2007) Tip Ciliophora Doflein, 1901 [Phylum Ciliophora Doflein, 1901]. In: Protisty: Rukovodstvo po zoologii, č. 2 [Protista: Handbook of Zoology, 2nd part], (Ed. A. F. Alimov). Nauka, St. Petersburg, 415–993 (in Russian with English summary)

Ji D., Wang Y. (2018) An optimized protocol of protargol staining for ciliated protozoa. *J. Eukaryot. Microbiol.* **65:** 705–708

Kahl A. (1930) Urtiere oder Protozoa I: Wimpertiere oder Ciliata (Infusoria) 1. Allgemeiner Teil und Prostomata. *Tierwelt Dtl.* **18:** 1–180

Kwon C. B., Vďačný P., Shazib S. U. A., Shin M. K. (2014) Morphology and molecular phylogeny of a new haptorian ciliate, *Chaenea mirabilis* sp. n., with implications for the evolution of the dorsal brush in haptorians (Ciliophora, Litostomatea). *J. Eukaryot. Microbiol.* **61:** 278–292

Lynn D. H. (2008) The Ciliated Protozoa. Characterization, Classification and Guide to the literature. 3rd ed. Springer, Dordrecht

Müller O. F. (1773) Vermium Terrestrium et Fluviatilium, seu Animalium Infusoriorum, Helminthicorum et Testaceorum, non Marinorum, Succincta Historia. Heineck & Faber, Havniae & Lipsiae

Müller O. F. (1786) Animalcula Infusoria Fluviatilia et Marina, quae Detexit, Systematice Descripsit et ad Vivum Delineari Curavit. Mölleri, Hauniae

Penard E. (1922) Études sur les Infusoires d'Eau Douce. Georg and Cie, Genève

Posada D. (2008) JModelTest: phylogenetic model averaging. *Mol. Biol. Evol.* **25:** 1253–1256

Rambaut A. (2009) FigTree v. 1.2.3. Available at http://tree.bio.ed.ac.uk/software/figtree/

Ronquist F., Teslenko M., van der Mark P., Ayres D. L., Darling A., Höhna S., Larget B., Liu L., Suchard M. A., Huelsenbeck J. P. (2012) MrBayes 3.2: efficient Bayesian phylogenetic inference and model choice across a large model space. *Syst. Biol.* **61:** 539–542

Schneider C. A., Rasband W. S., Eliceiri K. W. (2012) NIH Image to ImageJ: 25 years of image analysis. *Nat. Methods* **9:** 671–675

Sela I., Ashkenazy H., Katoh K., Pupko T. (2015) GUIDANCE2: accurate detection of unreliable alignment regions accounting for the uncertainty of multiple parameters. *Nucleic Acids Res.* **43:** W7–W14

Small E. B., Lynn D. H. (1981) A new macrosystem for the Phylum Ciliophora Doflein, 1901.

DOI: 10.4467/16890027AP.19.004.10835

BioSystems **14:** 387–401

Song W., Wilbert N. (1989) Taxonomische Untersuchungen an Aufwuschsciliaten (Protozoa, Ciliophora) im Poppelsdorfer Weiher, Bonn. *Lauterbornia* **3:** 1–221

Stokes A. C. (1885) Notices of new fresh-water infusoria. IV. *Am. Mon. Microsc. J.* **6:** 183–190

Švec F. (1897) Beiträge zur Kenntnis der Infusorien Böhmens. I. Die ciliaten Infusorien des Unterpocernitzer Teiches. *Bull. Int. Acad. Tchéque Sci.* **4:** 29–47

Vďačný P., Foissner W. (2012) Monograph of the dileptids (Protista, Ciliophora, Rhynchostomatia). *Denisia* **31:** 1–529

Vďačný P., Rataj M. (2017) Evaluation of systematic position of helicoprorodontids and chaeneids (Ciliophora, Litostomatea): an attempt to break long branches in 18S rRNA gene phylogenies. *J. Eukaryot. Microbiol.* **64:** 608–621

Vďačný P., Bourland W. A., Orsi W., Epstein S. S., Foissner W. (2011) Phylogeny and classification of the Litostomatea (Protista, Ciliophora), with emphasis on free-living taxa and the 18S rRNA gene. *Mol. Phylogenet. Evol.* **59:** 510–522

Vďačný P., Bourland W. A., Orsi W., Epstein S. S., Foissner W. (2012) Genealogical analyses of multiple loci of litostomatean ciliates (Protista, Ciliophora, Litostomatea). *Mol. Phylogenet. Evol.* **65:** 397–411

Vuxanovici A. (1963) Contributii la sistematica ciliatelor (Nota IV). *Studii Cerc. Biol. (Biol. Anim.)* **15:** 65–93 (in Rumanian with Russian and French summaries)

Wang Y., Ji D., Yin J. (2019) Morphology and phylogeny of two *Phialina* species (Ciliophora, Haptoria) from northern China. *Eur. J. Protistol.* **67:** 46–58

Wu L., Jiao X. X., Shen Z., Yi Z. Z., Li J. Q., Warren A., Lin X. F. (2017) New taxa refresh the phylogeny and classification of pleurostomatid ciliates (Ciliophora, Litostomatea). *Zool. Scr.* **46:** 245–253

Zhang Q., Simpson A., Song W. (2012) Insights into the phylogeny of systematically controversial haptorian ciliates (Ciliophora, Litostomatea) based on multigene analyses. *Proc. R. Soc. Lond. B Biol. Sci.* **279:** 2625–2635

Received on 29th April, 2019; revised on 7th June, 2019; accepted on 4th July, 2019

DOI: 10.4467/16890027AP.19.004.10835

Figures

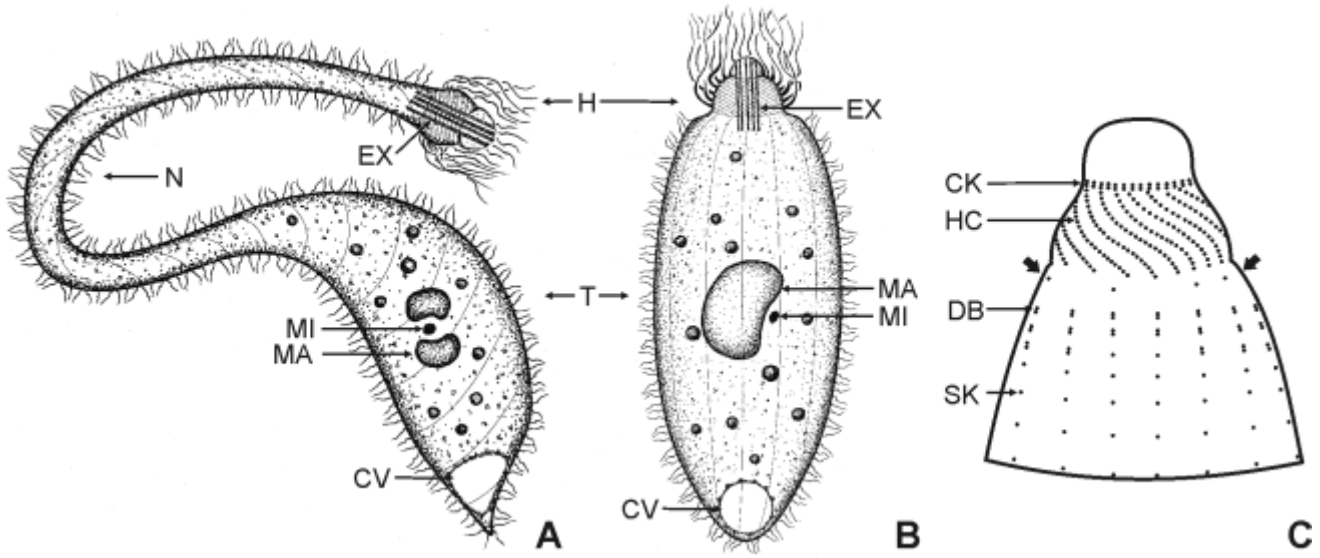

Fig. 1. A–C. Schematic diagrams of general body organization of *Lacrymaria* (A), *Phialina* (B) and

DOI: 10.4467/16890027AP.19.004.10835

Phialinides (C). Based on Dragesco and Dragesco-Kernéis 1986 (A, B) and Foissner 1988 (C). **(A)** *Lacrymaria* is characterized by a long, flexible and highly contractile neck, arising from the trunk and carrying the head. **(B)** *Phialina* does not have a distinct neck, and the head is thus attached directly to the trunk. **(C)** *Phialinides* differs from *Phialina* only by having a monokinetidal circle (paratene) between the head kineties and the dorsal brush (arrows). CK – circumoral kinety; CV – contractile vacuole; DB – dorsal brush; EX – extrusomes; H – head; HC – head kineties; MA – macronucleus; MI – micronucleus; N – neck; OB – oral bulge; SK – somatic kineties; T – trunk.

DOI: 10.4467/16890027AP.19.004.10835

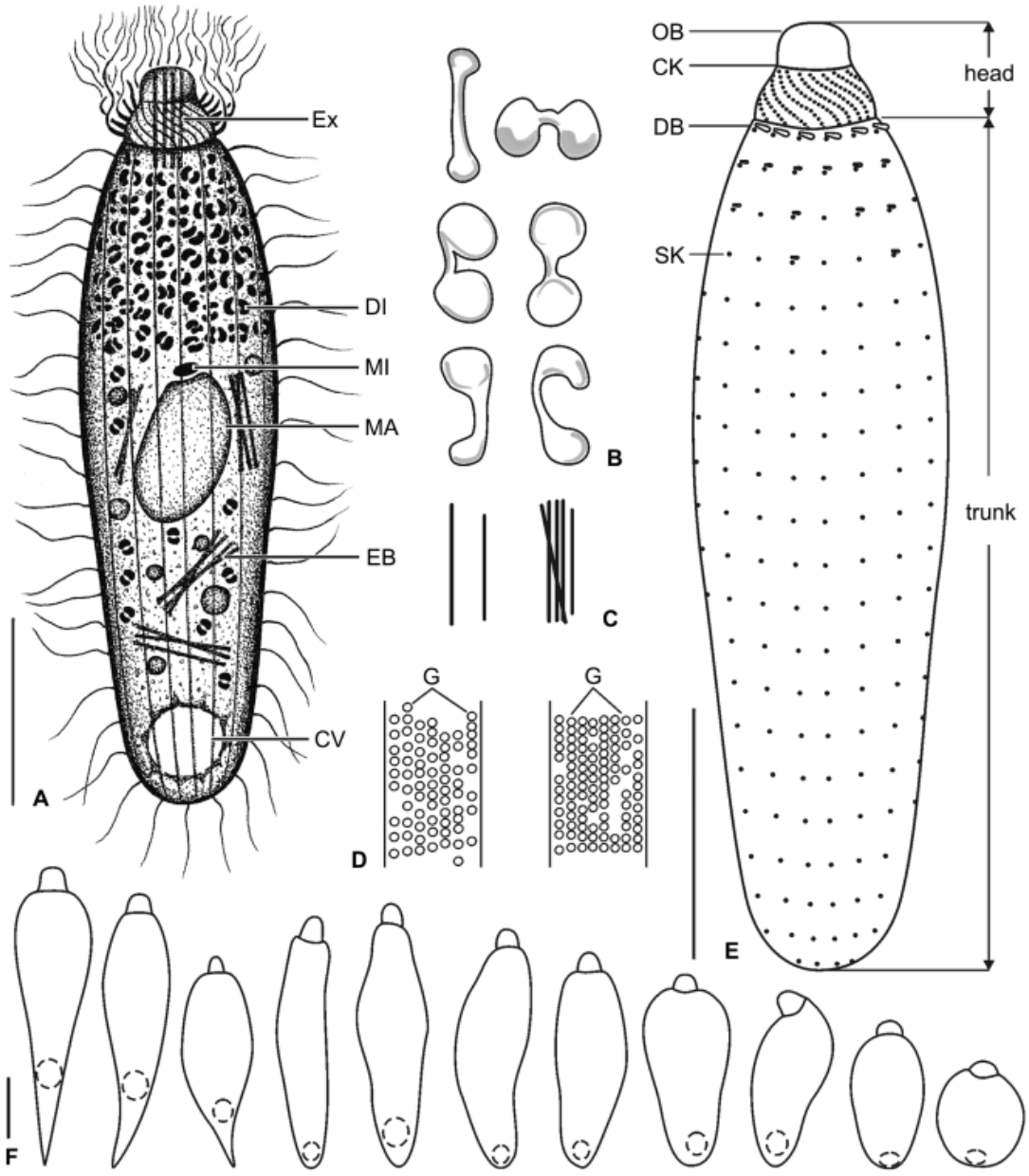

Fig. 2. A–F. *Phialina pupula* from life (A–D, F) and after protargol impregnation (E). **(A)** Overview of a representative semi-contracted specimen. **(B)** Details of dumbbell-shaped inclusions from various views. **(C)** Extrusomes are rod-shaped and about 10 μm long. **(D)** Surface view showing cortical granulation. **(E)** Ciliary pattern. **(F)** Variability of body shape in extended, semi-contracted and contracted cells. CK – circumoral kinety; CV – contractile vacuole; DB – dorsal brush; DI – dumbbell-shaped inclusions; EB – extrusome bundle; EX – extrusomes; G – cortical granules; OB – oral bulge; MA – macronucleus; MI – micronucleus; SK – somatic kineties. Scale bars: 20 μm.

DOI: 10.4467/16890027AP.19.004.10835

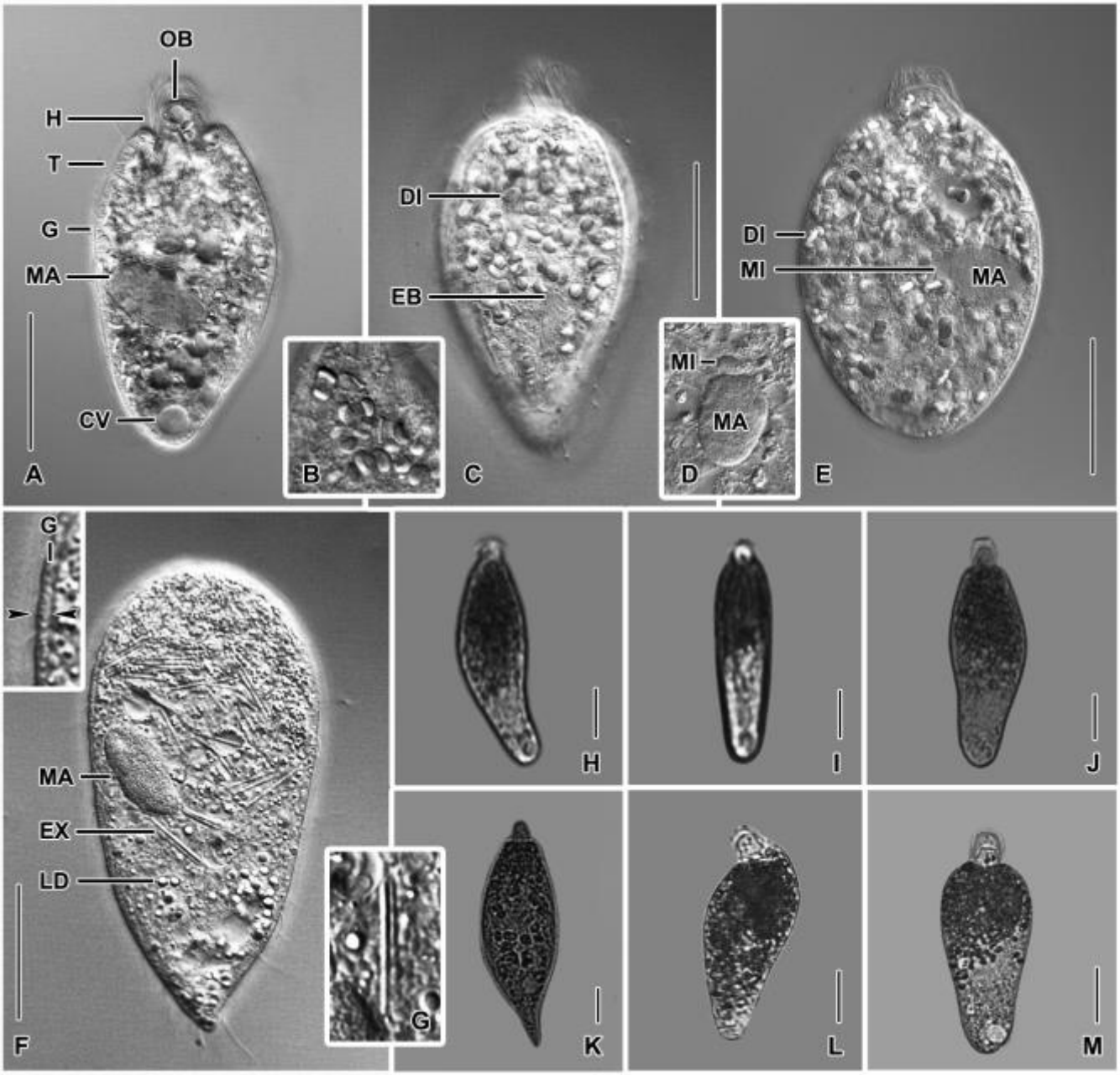

DOI: 10.4467/16890027AP.19.004.10835

Fig. 3. *Phialina pupula* from life under differential interference contrast (A–G) and bright field (H–M) illumination. **(A)** Overview of a semi-contracted specimen, showing the general body organization. The head is attached directly to the broadly fusiform trunk. Note that the contractile vacuole is located terminally due to the body contraction. The macronucleus is elliptical and situated slightly below the mid-body. **(B)** Detail of the highly refractive dumbbell-shaped inclusions scattered throughout the cytoplasm. **(C)** A semi-contracted specimen, showing an accumulation of the dumbbell-shaped inclusions in the anterior body half. **(D)** Detail of the nuclear apparatus. The macronucleus is elliptical, and the micronucleus is attached to the anterior pole of the macronucleus. **(E)** A contracted specimen, showing many refractive, dumbbell-shaped inclusions scattered throughout the cytoplasm and an elliptical macronucleus accompanied by a single micronucleus. **(F)** A strongly squeezed specimen, showing the nuclear apparatus, multiple extrusome bundles and some lipid droplets scattered throughout the cytoplasm. Left inset shows optical section through the cortex (opposed arrowhead), containing inconspicuous elliptical granules. **(G)** Detail of a cytoplasmic rod-shaped extrusome. **(H, J)** Fusiform, slightly curved cells with narrowly rounded posterior body end. **(I)** A cylindrical cell. **(K)** An extended, fusiform exemplar with tail-like posterior end. **(L)** A sigmoid cell with narrowly rounded ends. **(M)** A semi-contracted, obpyriform specimen with broadly rounded posterior body end. CV – contractile vacuole; DI – dumbbell-shaped inclusions; EB – extrusome bundles; EX – extrusomes; G – cortical granules; H – head; LD – lipid droplets; MA – macronucleus; MI – micronucleus; OB – oral bulge; T – trunk. Scale bars: 20 μm.

DOI: 10.4467/16890027AP.19.004.10835

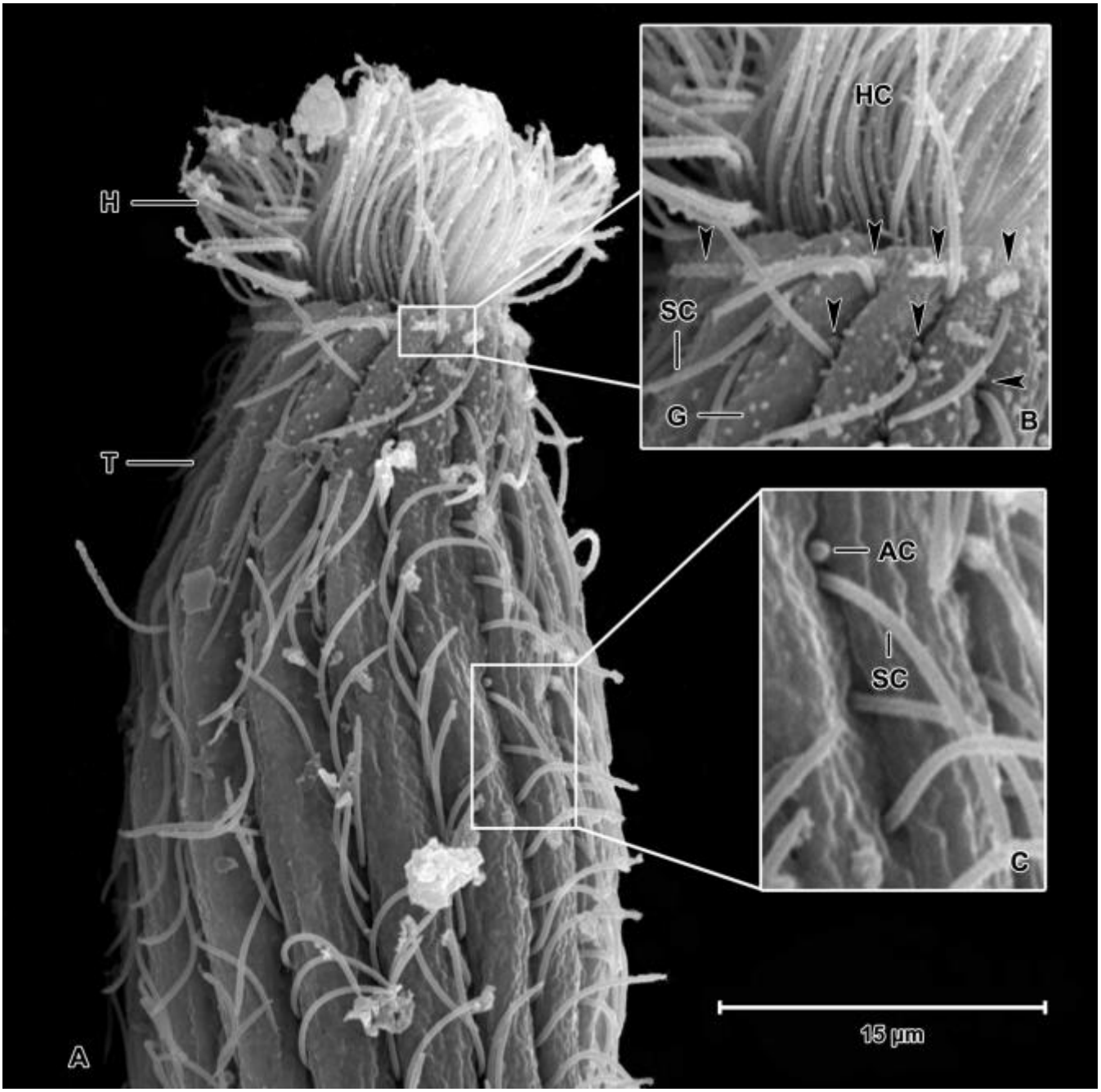

DOI: 10.4467/16890027AP.19.004.10835

Fig. 4. *Phialina pupula* in the scanning electron microscope (SEM). **(A)** Detail of the anterior body half. The head is localized at the anterior body end and is attached directly to the trunk, as typical of the genus *Phialina*. The head is covered by very narrowly spaced cilia arranged in helically extending rows. Note that the cortex of the trunk is distinctly furrowed by slightly helically extending ciliary rows. According to protargol preparations, each somatic ciliary row has two to five brush dikinetids at its anterior end (see Fig. 2E). SEM observations show that the anterior basal body of a brush dikinetid bears a minute to short cilium or is unciliated, while the posterior basal body bears an ordinary somatic cilium. Therefore, the brush is very difficult to recognize in the SEM and in vivo. **(B)** Detail of the anterior end of somatic ciliary rows, showing that the anterior basal body of a brush dikinetid bears a short cilium (arrowheads) or is unciliated. The posterior basal body of a brush dikinetid bears an ordinary somatic cilium. Such an inconspicuous brush is a typical feature of lacrymariids and also of the possibly related chaeneids. **(C)** Detail of a somatic ciliary row, showing a dikinetid (dividing basal bodies) followed by monokinetids that bear ordinary cilia. As typical for haptorians, the anterior cilium of dividing basal bodies is short and stump-like while the posterior cilium is ordinarily long. AC – anterior stump-like cilium of dividing basal bodies; G – tips of cortical granules; H – head; HC – head cilia; SC – somatic cilia; T – trunk.

DOI: 10.4467/16890027AP.19.004.10835

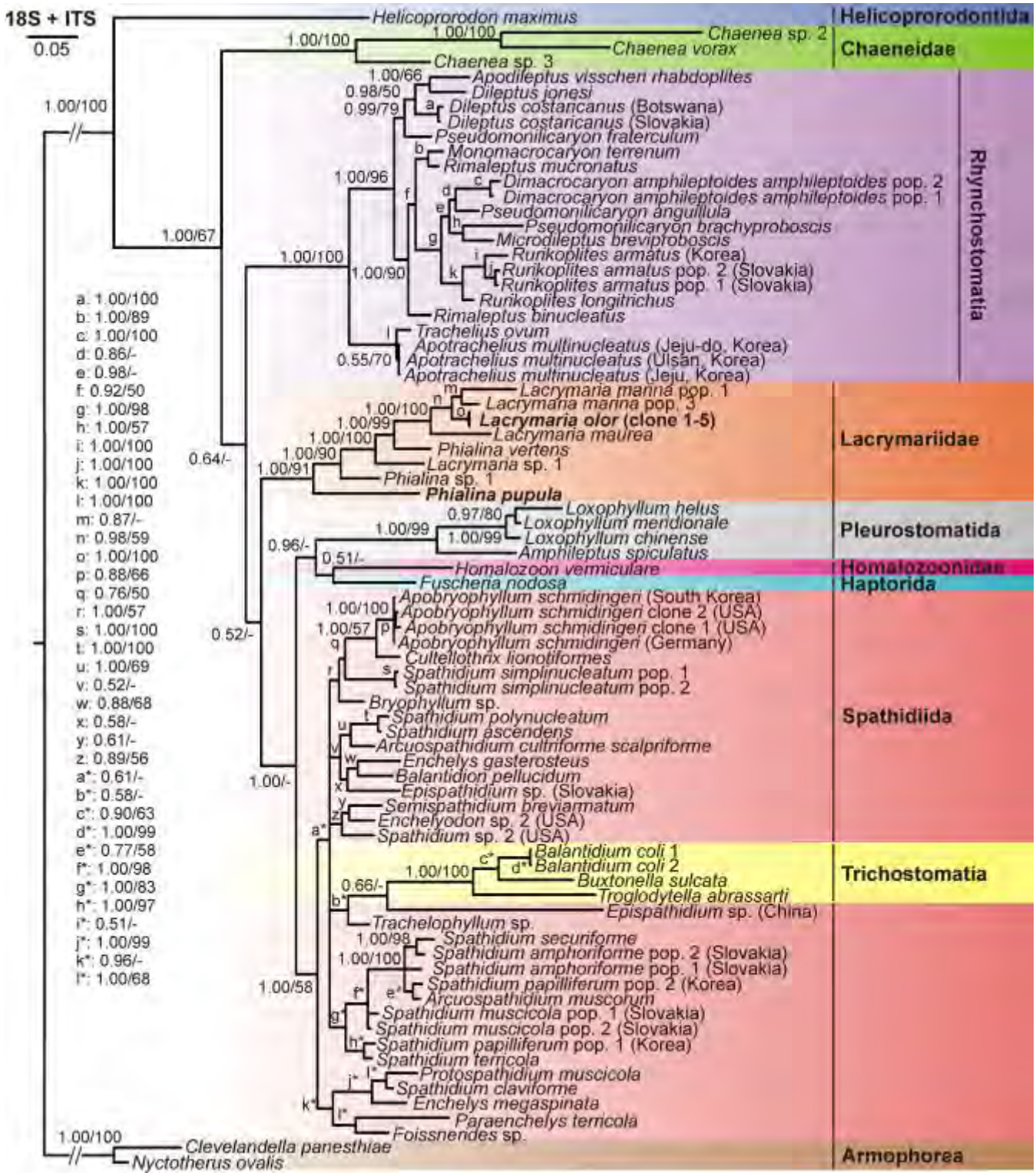

DOI: 10.4467/16890027AP.19.004.10835

Fig. 5. Phylogeny based on the 18S rRNA gene and the ITS1-5.8S-ITS2 region of 80 litostomatean taxa and two armophoreans serving as outgroup (CON-lit alignment). Posterior probabilities for the Bayesian inference and bootstrap values for maximum likelihood were mapped onto the 50%-majority rule Bayesian consensus tree. Note that monophyly of the family Lacrymariidae is moderately to strongly statistically supported. Sequences in bold face were obtained during this study. The scale bar indicates five substitutions per one hundred nucleotide positions. For GenBank accession numbers, see Supplementary Table S3.

DOI: 10.4467/16890027AP.19.004.10835

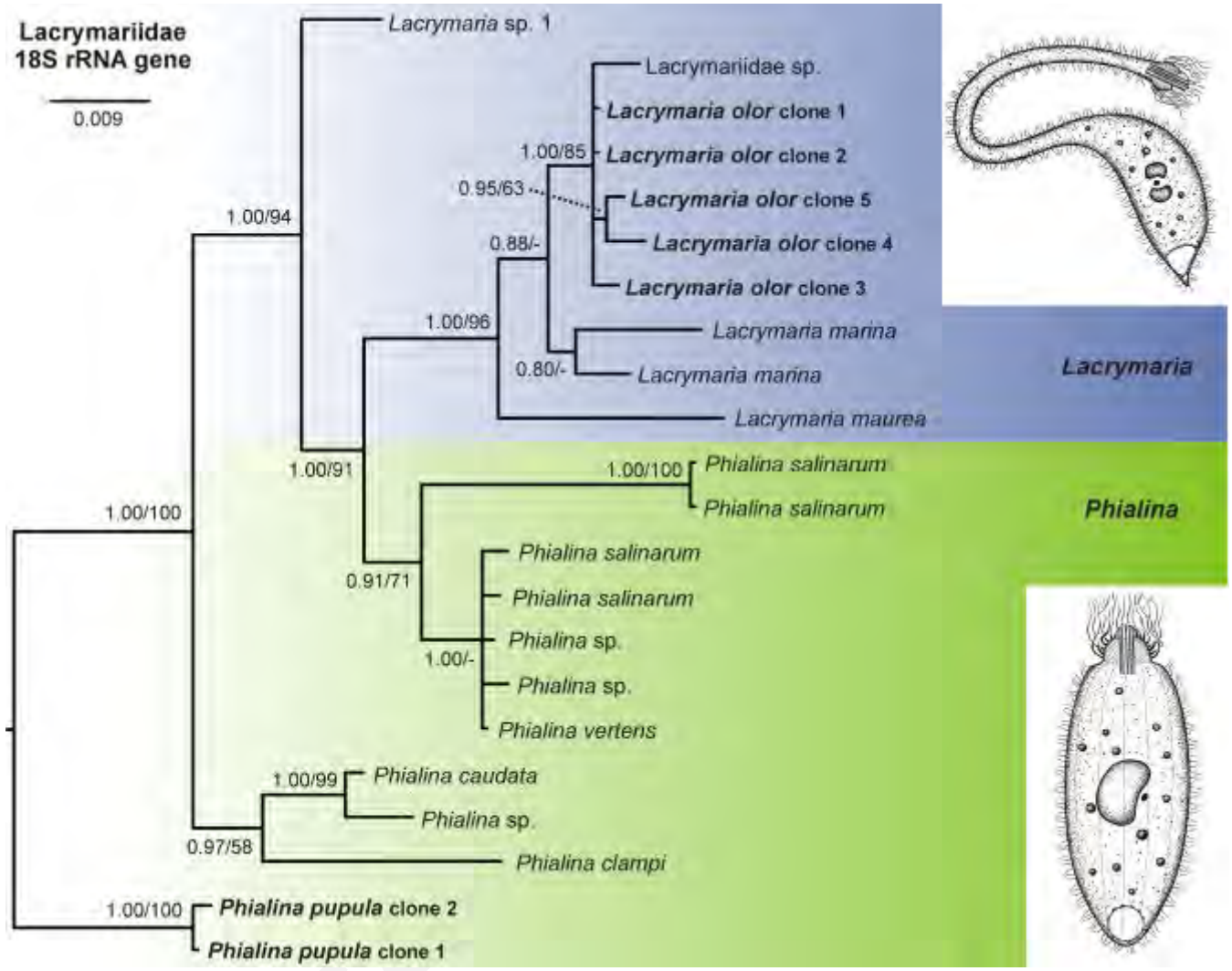

Fig. 6. Phylogeny based on the 18S rRNA gene of 22 taxa from the family Lacrymariidae (18S-lac1 alignment). Note that the genus *Phialina* is paraphyletic and contains the polyphyletic genus *Lacrymaria*. Posterior probabilities for the Bayesian inference and bootstrap values for maximum likelihood were mapped onto the 50%-majority rule ML tree. Sequences in bold were obtained during this study. The scale bar indicates nine substitutions per one thousand nucleotide positions.

DOI: 10.4467/16890027AP.19.004.10835

Table 1. Morphometric data on *Phialina pupula* (Boise population).

Characteristics[a]	Mean	M	SD	SE	CV	Min	Max	*n*
Body, length	75.3	74.5	14.2	2.5	18.8	53.0	115.0	32
Body, width	26.4	26.5	6.1	1.1	23.1	17.0	42.0	32
Body length:width, ratio	2.9	2.8	0.6	0.1	20.6	1.7	4.4	32
Head, height	8.4	9.0	1.2	0.2	13.9	5.0	11.0	32
Head, width	6.1	6.0	0.9	0.2	15.4	5.0	8.0	31
Anterior body end to macronucleus, distance	34.9	35.0	11.0	2.0	31.5	10.0	59.0	32
Macronucleus, length	15.2	15.0	2.6	0.5	17.1	10.0	20.0	32
Macronucleus, width	9.5	9.0	2.2	0.4	23.5	5.0	16.0	32
Extrusome, length	9.7	10.0	0.8	0.2	8.1	8.0	11.0	25
Somatic ciliary rows, number	15.0	16.0	1.3	0.3	8.9	12.0	16.0	20
Somatic ciliary rows, distance in between	3.9	4.0	0.5	0.1	13.0	3.0	4.5	16
Kinetids in a ciliary row, total number	21.8	21.0	5.7	1.7	26.3	13.5	33.0	12
Kinetids in a ciliary row, distance in between	3.2	3.0	0.5	0.1	16.6	2.0	4.0	18
Brush dikinetids in a kinety, number	3.7	3.8	1.1	0.5	29.1	2.0	5.0	6

[a] Data based on protargol-impregnated and semi-contracted to extended specimens. Measurements in µm. CV, coefficient of variation (%); M – median; Max – maximum; Mean – arithmetic mean; Min – minimum; *n* – number of individuals investigated; SD – standard deviation; SE – standard error of arithmetic mean.

DOI: 10.4467/16890027AP.19.004.10835

Supplementary Table S1. Characterization of new 18S rRNA gene and ITS region sequences obtained during this study.

Taxon	Collection site	Clone No.	18S rRNA gene			ITS1-5.8S-ITS2 region[a]		
			Length (nt)	GC (%)	GenBank entry	Length (nt)	GC (%)	GenBank entry
Phialina pupula	Sediments from the floodplain area of the Boise River near the Glenwood Bridge, Boise, Idaho, U.S.A.	1	1636	42.85	MN030551	1190	43.36	MN030617
		2	1636	42.72	MN030552	–	–	–
Lacrymaria olor	Water and sediments from the shore area of a pond at the Julia Davis Park, 700 S. Capitol Blvd. Boise, Idaho, U.S.A.	1	1642	42.75	MN030553	1293	42.30	MN030618
		2	1642	42.75	MN030554	1293	42.30	MN030619
		3	1642	42.75	MN030555	1293	42.23	MN030620
		4	1642	42.69	MN030556	1293	42.23	MN030621
		5	1642	42.69	MN030557	1293	42.23	MN030622
		6	–	–	–	1293	42.23	MN030623
		7	–	–	–	1293	42.23	MN030624
		8	–	–	–	1293	42.23	MN030625

[a] These sequences also contain a variably long 5'-end of the 28S rRNA gene.

DOI: 10.4467/16890027AP.19.004.10835

Supplementary Table S2. Characterization and parameterization of the GTR evolutionary models of the alignments analyzed.

Characteristics[a]	Alignment									
	18S-lit1	18S-lit2	18S-lac1	18S-lac2	ITS-lit1	ITS-lit2	ITS-lac1	ITS-lac2	CON-lit[c]	CON-lac[d]
No. of taxa	129	129	22	22	91	91	17	17	82	12
No of characters	1349	1527	1487	1507	210	356	299	371	1883	1883
Cutoff value[b]	0.93	–	0.93	–	0.93	–	0.93	–	–	–
A	0.2817	0.2894	0.3010	0.2992	0.3249	0.3673	0.3508	0.3543	0.3153	0.3103
C	0.1843	0.1790	0.1822	0.1825	0.1852	0.1994	0.1830	0.1787	0.1829	0.1789
G	0.2470	0.2359	0.2398	0.2378	0.2165	0.1496	0.2062	0.1866	0.2226	0.2339
T	0.2870	0.2957	0.2769	0.2806	0.2734	0.2837	0.2600	0.2804	0.2792	0.2770
[AC]	1.6547	1.6126	2.3799	2.4903	0.9967	1.7559	3.6876	3.1737	1.8846	2.6614
[AG]	4.0289	3.9554	4.0557	3.8830	4.6597	2.5996	4.5027	3.1603	3.1053	3.3593
[AT]	2.5551	2.6210	3.4924	3.3830	2.8135	2.5847	5.1508	4.4708	3.0859	4.6261
[CG]	0.6655	0.7834	1.2918	1.1898	0.3135	0.7256	0.0035	0.0013	0.6617	0.8501
[CT]	6.0464	6.2297	5.0269	6.2357	9.6946	5.3820	8.5199	7.3266	6.8550	7.2045
[GT]	1.0000	1.0000	1.000	1.0000	1.0000	1.0000	1.0000	1.0000	1.0000	1.0000
I	0.4380	0.3950	0.7340	0.6690	0.3380	0.1580	0.5510	0.2120	0.3830	0.0000
Γ	0.3420	0.3660	0.7390	0.5060	0.5370	0.5400	0.6890	0.5080	0.4110	0.0170

[a] The best fitting evolutionary models were selected for each dataset under the Akaike information criterion in jModelTest. A, C, G, T, base frequencies; [AC], [AG], [AT], [CG], [CT], [GT], rate substitution matrices; I, proportion of invariable sites; Γ, gamma distribution shape parameter.
[b] Unreliably aligned columns were removed from the alignment at the cutoff value of 0.93. Dash indicates no masking strategy.
[c] The CON-lit dataset was created by combining the 18S-lit2 and the ITS-lit2 alignment.
[d] The CON-lac dataset was created by combining the 18S-lac2 and the ITS-lac2 alignment.

DOI: 10.4467/16890027AP.19.004.10835

Supplementary Table S3. List of ciliate taxa with GenBank accession numbers of corresponding 18S rRNA gene sequences and ITS1-5.8S-ITS2 region sequences included in phylogenetic analyses. Newly obtained sequences are in bold face.

Taxon	GenBank entry		Taxon	GenBank entry	
	18S rRNA gene	ITS region		18S rRNA gene	ITS region
ARMOPHOREA (OUTGROUP)			*Rimaleptus binucleatus*	KJ680552	MF288137
Clevelandella panesthiae	KC139719	KC460347	*Rimaleptus mucronatus*	HM581675	JX070865
Nyctotherus ovalis	AJ222678	AJ006714	*Rurikoplites armatus* (Korea)	MF288145	MF288138
CHAENEIDAE			*Rurikoplites armatus* pop. 1 (Slovakia)	KP868771	KP868778
Chaenea sp. 2	MF474336	MF474336	*Rurikoplites armatus* pop. 2 (Slovakia)	KP868772	KP868779
Chaenea sp. 3	MF474337	MF474337	*Rurikoplites longitrichus*	MF288146	MF288139
Chaenea vorax	MF474338	MF474364	*Trachelius ovum*	KJ680553	MF288140
HAPTORIDA			SPATHIDIIDA		
Fuscheria nodosa	MG264143	MG264149	*Apobryophyllum schmidingeri* clone 1 (USA)	MG264145	MG264152
HELICOPRORODONTIDA			*Apobryophyllum schmidingeri* clone 2 (USA)	MG264146	MG264153
Helicoprorodon maximus	KM222102	KM222061	*Apobryophyllum schmidingeri* (Germany)	JF263441	JX070870
HOMALOZOONIDAE			*Apobryophyllum schmidingeri* (South Korea)	KY556646	KY556653
Homalozoon vermiculare	MF474342	MF474368	*Arcuospathidium cultriforme scalpriforme*	KT246076	MG264154
LACRYMARIIDAE			*Arcuospathidium muscorum*	KT246077	KT246091
Lacrymaria marina pop. 1	FJ876975	DQ811088	*Balantidion pellucidum*	JF263444	JX070880
Lacrymaria marina pop. 3	MF474343	MF474369	*Bryophyllum* sp.	KT246078	KT246092
Lacrymaria maurea	MF474344	MF474370	*Cultellothrix lionotiformes*	JF263445	JX070879
***Lacrymaria olor* clone 1**	**MN030553**	**MN030618**	*Enchelyodon* sp. 2	JF263446	JX070874
***Lacrymaria olor* clone 2**	**MN030554**	**MN030619**	*Enchelys gasterosteus*	JF263447	JX070875
***Lacrymaria olor* clone 3**	**MN030555**	**MN030620**	*Enchelys megaspinata*	KY556648	KY556655
***Lacrymaria olor* clone 4**	**MN030556**	**MN030621**	*Epispathidium* sp. (Slovakia)	KT246081	KT246094
***Lacrymaria olor* clone 5**	**MN030557**	**MN030622**	*Epispathidium* sp. (China)	MF474339	MF474366

DOI: 10.4467/16890027AP.19.004.10835

Lacrymaria sp. 1	MF474345	MF474371	*Foissnerides* sp.	MF474340	MF474367
***Phialina pupula* clone 1**	**MN030551**	**MN030617**	*Paraenchelys terricola*	MG264147	MG264155
Phialina sp. 1	MF474346	MF474372	*Protospathidium muscicola*	JF263449	JX070876
Phialina vertens	MF474348	MF474374	*Semispathidium breviarmatum*	JF263450	JX070873
PLEUROSTOMATIDA			*Spathidium amphoriforme* pop. 1 (Slovakia)	KT246079	MG264156
Amphileptus spiculatus	KM025129	KU925883	*Spathidium amphoriforme* pop. 2 (Slovakia)	KT246080	KT246093
Loxophyllum chinense	JN974455	KU925880	*Spathidium ascendens*	KY556643	KY556651
Loxophyllum helus	KT246084	KT246095	*Spathidium claviforme*	KT246086	MG264157
Loxophyllum meridionale	KC469985	KU925881	*Spathidium muscicola* pop. 1 (Slovakia)	KT246087	KT246096
RHYNCHOSTOMATIA			*Spathidium muscicola* pop. 2 (Slovakia)	KT246088	KT246097
Apodileptus visscheri rhabdoplites	HM581678	JX070869	*Spathidium papilliferum* pop. 1 (Korea)	KY556645	KY556652
Apotrachelius multinucleatus (Jeju, Korea)	MF288143	MF288134	*Spathidium papilliferum* pop. 2 (Korea)	KY556649	KY556656
Apotrachelius multinucleatus (Jeju-do, Korea)	KJ680554	MF288141	*Spathidium polynucleatum*	KY556647	KY556654
Apotrachelius multinucleatus (Ulsan, Korea)	MF288147	F288142	*Spathidium securiforme*	KY556642	KY556650
Dileptus costaricanus (Botswana)	HM581679	JX070868	*Spathidium simplinucleatum* pop. 1	KT246089	KT246098
Dileptus costaricanus (Slovakia)	KP868765	KP868773	*Spathidium simplinucleatum* pop. 2	KT246090	KT246099
Dileptus jonesi	MF288144	MF288135	*Spathidium* sp. 2 (USA)	JF263451	JX070877
Dimacrocaryon amph. amphileptoides pop. 1	KP868766	KP868774	*Spathidium terricola*	KT246082	MG264158
Dimacrocaryon amph, amphileptoides pop. 2	KP868767	KP868775	TRICHOSTOMATIA		
Microdileptus breviproboscis	KP868768	KP868776	*Balantidium coli* 1	AM982722	AM982724
Monomacrocaryon terrenum	HM581674	JX070864	*Balantidium coli* 2	AM982723	AM982726
Pseudomonilicaryon anguillula	KJ680551	MF288136	*Buxtonella sulcata*	KP016718	KP016716
Pseudomonilicaryon brachyproboscis	KP868769	KP868777	*Troglodytella abrassarti*	AB437346	EU680313
Pseudomonilicaryon fraterculum	HM581677	JX070867	*Trachelophyllum* sp.	JF263452	JX070878